Extended Finite Element Analysis of Injection-induced Seismicity on a Rate-and-State Fault

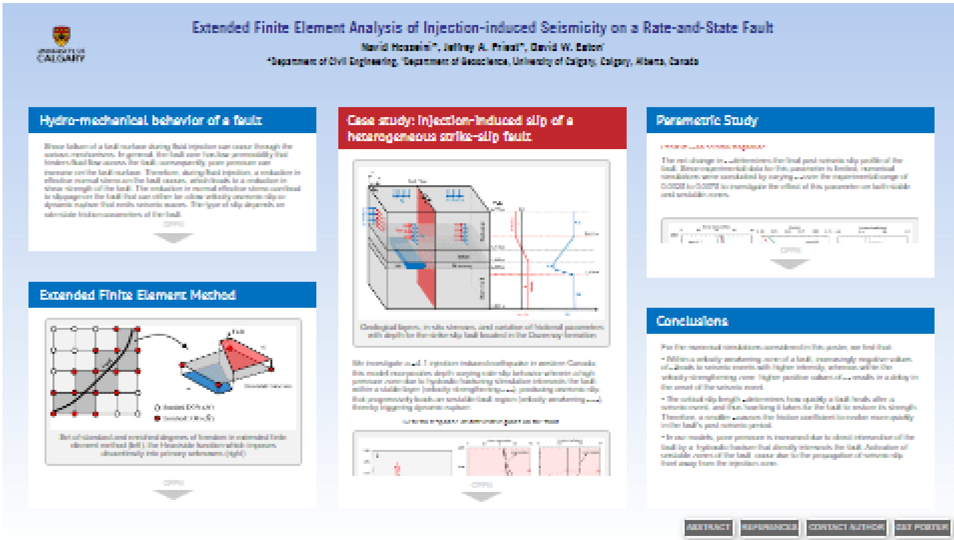

Navid Hosseini*, Jeffrey A. Priest*, David W. Eaton'

*Department of Civil Engineering, 'Department of Geoscience, University of Calgary, Calgary, Alberta, Canada

PRESENTED AT:

HYDRO-MECHANICAL BEHAVIOR OF A FAULT

Shear failure of a fault surface during fluid injection can occur through the various mechanisms. In general, the fault core has low permeability that hinders fluid flow across the fault; consequently, pore pressure can increase on the fault surface. Therefore, during fluid injection, a reduction in effective normal stress on the fault occurs, which leads to a reduction in shear strength of the fault. The reduction in normal effective stress can lead to slippage on the fault that can either be a low-velocity aseismic slip or dynamic rupture that emits seismic waves. The type of slip depends on rate-state friction parameters of the fault.

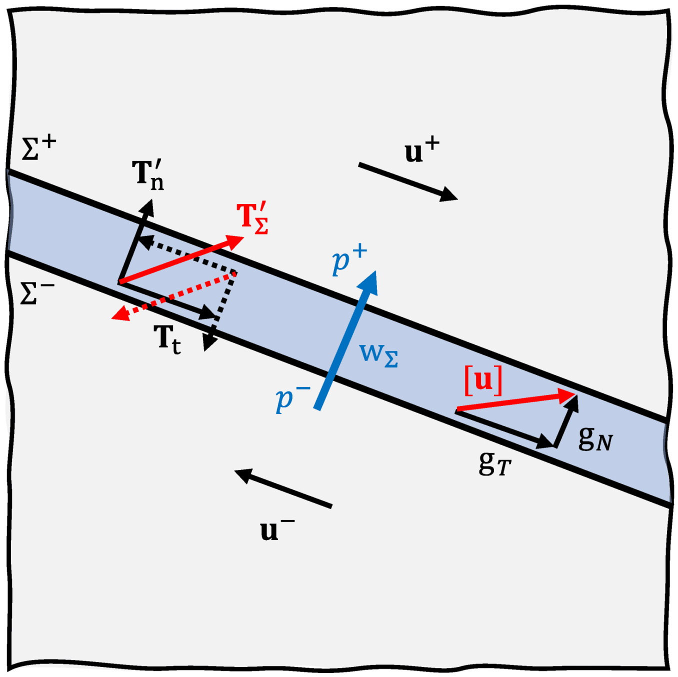

Schematic representation of a shear-tensile fault surface: effective traction vector ($\mathbf{T}'_{\Sigma}$) ; normal fluid velocity (w_{Σ}); displacement jump ($[\mathbf{u}]$) across the fault

Coulomb's frictional law:
According to Coulomb's frictional law, the shear strength (T_f) of fault can be given by

$$T_f = \mu|T_n'| + c$$

μ: coefficient of friction,
c: cohesive strength.
If the magnitude of shear stress on the fault is less than its shear strength, $|T_t| < T_f$then no relative movement parallel to the fault faces occurs (*stick state*). If $|T_t| = T_f$the fault slips and there is a relative movement between faces of the fault (*slip state*).

Rate-and-state friction:
For a rate-and-state friction model the coefficient of friction along the fault is function of slip rate (V) and state variable (θ) given by

$$\mu = \mu_0 + a\ln\left(\frac{V}{V_0}\right) + b\ln\left(\frac{\theta}{\theta_0}\right), \;\; \text{where} \;\; \dot{\theta} = 1 - \frac{V\theta}{D_c}$$

μ_0: steady-state friction coefficient at the reference slip rate V_0,
D_c: characteristic slip length,
$\theta_0 = D_c/V_0$: reference state variable.
Parameter a controls the change in the coefficient of friction due to a change in slip rate,
Parameter b captures the evolution of the contact population driven by slip.

EXTENDED FINITE ELEMENT METHOD

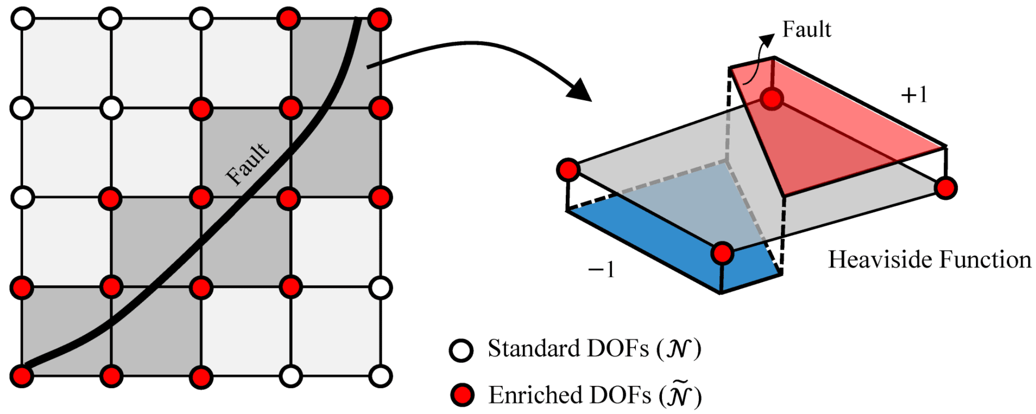

Set of standard and enriched degrees of freedom in extended finite element method (left), the Heaviside function which imposes discontinuity into primary unknowns (right)

In the X-FEM approach, the influence of the fault is captured by adding extra degrees of freedom to individual elements intersected by the discontinuity and the conventional FEM approximation is enriched with an appropriate function. To capture the jump in displacement and pressure fields resulting from a fault, the Heaviside function $H(\mathbf{x})$ is typically used as an appropriate enrichment function. Then, the approximation of the displacement or pressure fields can be written as

$$\mathbf{u}(\mathbf{x},t) \simeq \sum N_I(\mathbf{x})\bar{u}_I(t) + \sum N_I(\mathbf{x})(H(\mathbf{x}) - H(\mathbf{x}_I))\tilde{u}_I(t)$$

$\bar{u}_I(t)$: the nodal unknowns,
$\tilde{u}_I(t)$: the enriched nodal degrees of freedom,
$N_I(\mathbf{x})$: standard FEM shape functions.

CASE STUDY: INJECTION-INDUCED SLIP OF A HETEROGENEOUS STRIKE-SLIP FAULT

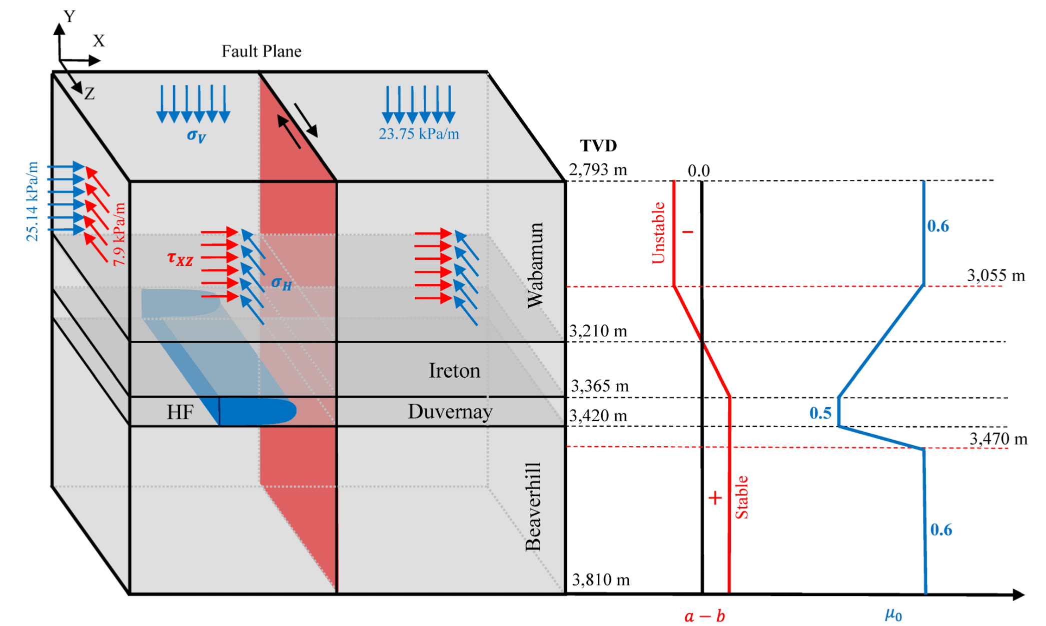

Geological layers, in-situ stresses, and variation of frictional parameters with depth for the strike-slip fault located in the Duvernay formation

We investigate a M_w 4.1 injection-induced earthquake in western Canada; this model incorporates depth-varying rate-slip behavior wherein a high-pressure zone due to hydraulic fracturing stimulation intersects the fault within a stable layer (velocity-strengthening $a-b>0$), producing aseismic slip that progressively loads an unstable fault region (velocity-weakening $a-b<0$), thereby triggering dynamic rupture.

General response of different regions on the fault

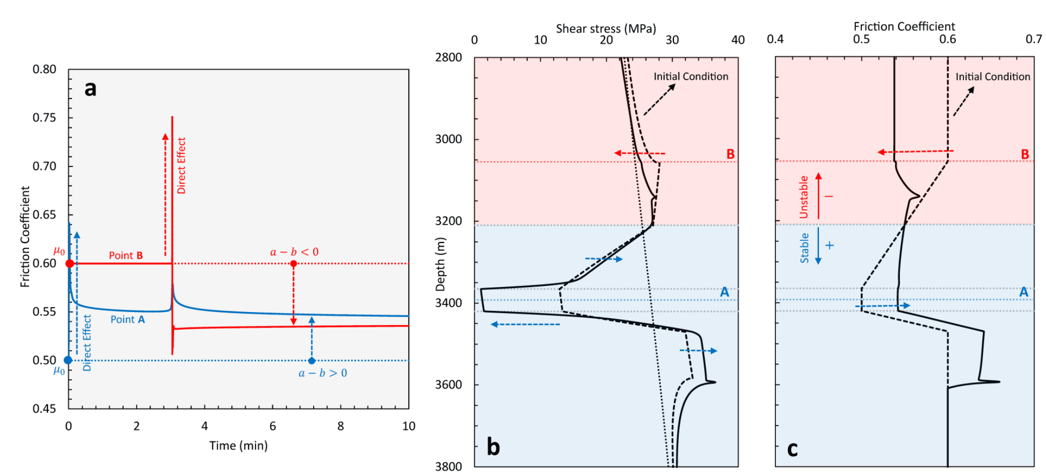

(**a**) time history of friction coefficient, profiles of (**b**) shear stress, and (**c**) friction coefficient along the fault at time 30 min.

Point A: The fault surface is initially at a steady-state sliding velocity, where the coefficient of friction is μ_0. After imposing HF pressure, the sliding rate is increased at point A, which was initially in a slip state; consequently, the coefficient of friction instantaneously increases, which is called direct effect and is controlled by the parameter a. As the fault surface moves, the slip rate decreases to its initial value and the direct-effect decreases over time. Meanwhile, the state variable evolves to a new steady-state value, resulting in a net increase in friction coefficient for point A. Specifically, the friction coefficient increases from an initial value of 0.5 to a higher value due to velocity-strengthening behaviour. As the pore pressure rises abruptly at point A, the effective stress drops, leading to a net decrease in shear stress over the Duvernay layer. It is noted that the main reason for shear stress relaxation over the Duvernay layer is the increase in pore pressure.

Point B: this point is initially in a stick state and is located in the vicinity of a stress concentration ahead of the rupture front. The stress concentration is generated due to high slip rates at the rupture fronts. As the rupture front propagates up the fault, the available shear stress at point B overcomes the static shear strength after which the fault at this point starts to slip in an unstable manner, arrested finally by the upper edge of the fault. The friction coefficient after 30 min is lower than its initial value (0.6) due to velocity-weakening behaviour. Since the effective stress remains constant, a drop in shear stress occurs at this point after the seismic event. Thus, the main reason for the drop in shear stress in the unstable zone is not the increase in pore pressure but the propagation of the rupture front.

PARAMETRIC STUDY

Effect of $a - b$ on seismic magnitude:

The net change in $a - b$ determines the final post-seismic slip profile of the fault. Since experimental data for this parameter is limited, numerical simulations were conducted by varying $a - b$ over the experimental range of 0.0025 to 0.0075 to investigate the effect of this parameter on both stable and unstable zones.

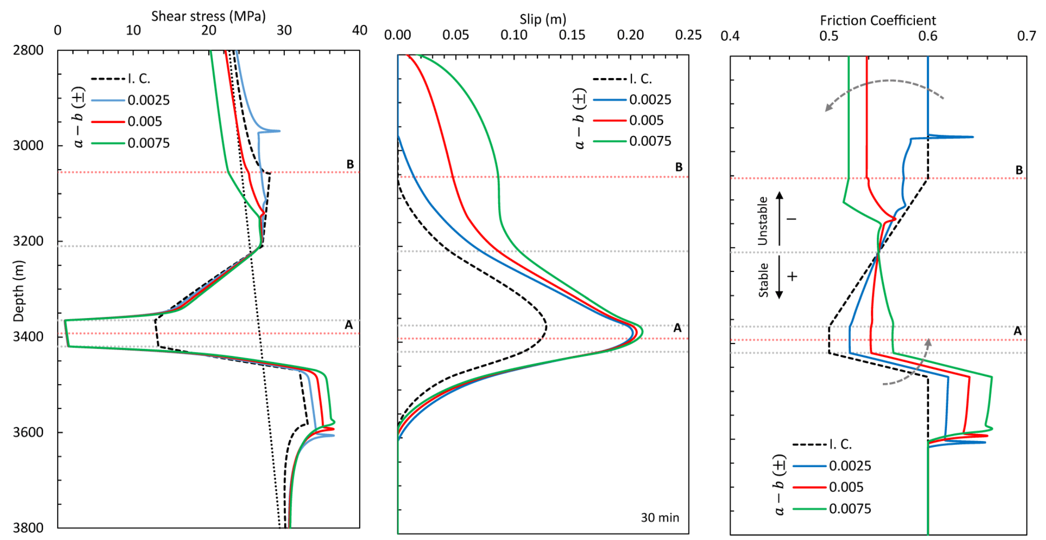

Distribution of shear stress, slip, and friction coefficient along the fault at time 30 min

As the magnitude of $a - b$ increases in unstable zone, a larger reduction in the friction coefficient after the seismic event occurs (point B), which corresponds to a larger reduction in shear stress over this zone. The magnitude of the jump in slip, as well as the corresponding seismic magnitude, is larger for higher $a - b$ values in unstable zone.

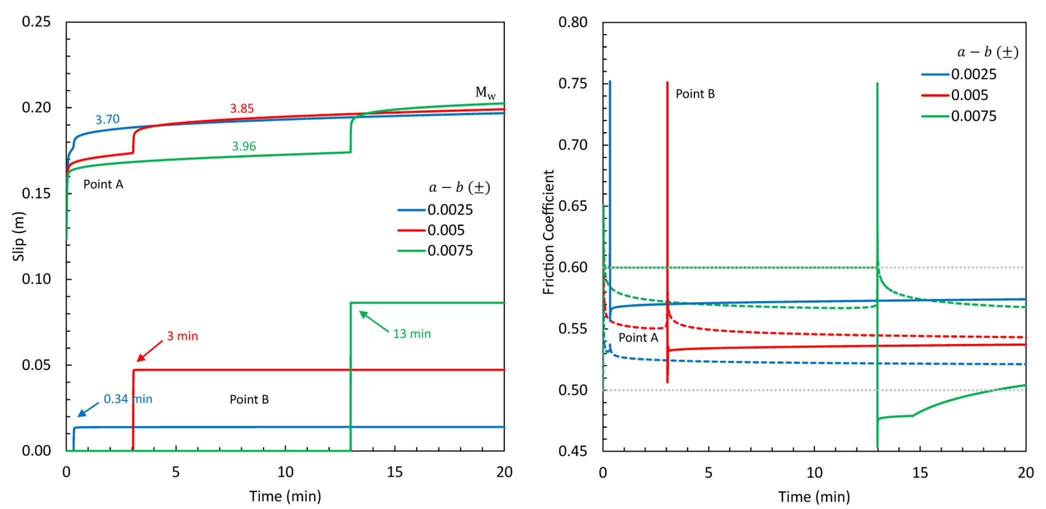

Time history for slip and friction coefficient at two points on the fault

A higher $a - b$ in the unstable zone leads to a seismic event occurring with a higher intensity, while a higher $a - b$ in the stable zone results in a delay in the onset of the seismic event.

Effect of D_c parameter on fault healing:

In the rate-and-state friction law, the critical slip length D_c relates to the rate of fault healing process, or the time required for the fault to regain its strength after a seismic event. Thus, lower D_c parameter leads to faster evolution in friction coefficient in the post-seismic transient response of the fault.

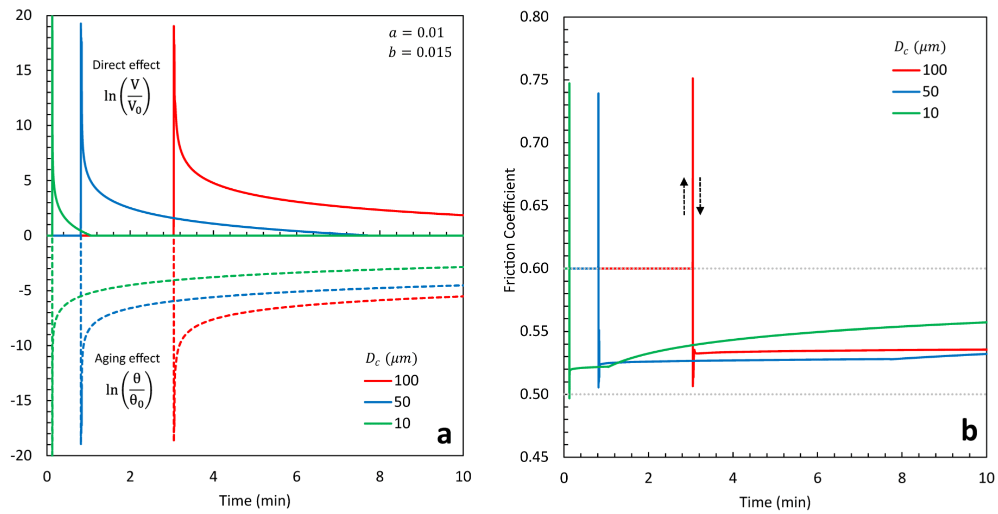

Time history for (**a**) direct-effect and aging terms of the rate-and-state model (**b**) friction coefficient at point B

CONCLUSIONS

For the numerical simulations considered in this poster, we find that:

• Within a velocity-weakening zone of a fault, increasingly negative values of $a - b$leads to seismic events with higher intensity, whereas within the velocity-strengthening zone higher positive values of $a - b$ results in a delay in the onset of the seismic event.

• The critical slip length D_c determines how quickly a fault heals after a seismic event, and thus how long it takes for the fault to restore its strength. Therefore, a smaller D_c causes the friction coefficient to evolve more quickly in the fault's post-seismic period.

• In our models, pore pressure is increased due to direct intersection of the fault by a hydraulic fracture that directly intersects the fault. Activation of unstable zones of the fault occur due to the propagation of seismic slip front away from the injection zone.

ABSTRACT

A poro-elastic model is developed to simulate the behavior of a rate-and-state fault during fluid injection. The hydro-mechanical behavior of the fault is coupled with the poro-elastic behavior of the surrounding porous formation. The fault rheology is embedded into the governing equations of Biot's theory for poro-elastic media, and the penalty method is used to impose the contact constraints for the fault. The presence of a fault induces some discontinuities in the solid displacement and fluid pressure fields, and the extended finite element method (X-FEM) is used for an accurate representation of these discontinuities by enriching the standard finite element approximation of the field variables with additional degrees of freedom for elements intersected by the fault. Finally, several parametric studies are conducted to investigate the influence of frictional parameters of the fault, as well as poro-elastic properties of the surrounding rock, on the response of a heterogeneous fault located in western Canada; and the results show that the difference a-b for rate-state parameters and hydraulic diffusivity of formation are the main factors which determine the intensity and occurrence time of seismic events.

REFERENCES

Eyre T. S., Eaton D. W., Garagash D. I., Zecevic M., Venieri M., Weir R., & Lawton D. C. (2019). **The role of aseismic slip in hydraulic fracturing–induced seismicity**. *Science advances*, 5(8), eaav7172.

Liu F., & Borja R.I. (2009). **An extended finite element framework for slow-rate frictional faulting with bulk plasticity and variable friction**. *International Journal for Numerical and Analytical Methods in Geomechanics*, 33(13):1535–1560.

Cueto-Felgueroso L., Vila C., Santillá, D., & Mosquera J. C. (2018). **Numerical modeling of injection-induced earthquakes using laboratory-derived friction laws**. *Water Resources Research*, 54(12), 9833-9859.

Jha B., & Juanes R. (2014). **Coupled multiphase flow and poromechanics: A computational model of pore pressure effects on fault slip and earthquake triggering**. *Water Resources Research*, 50(5):3776–3808.